Geochemical and petrogenetic study of Proterozoic Sewariya and Govindgarh granitoids from South Delhi Fold Belt

Soumya Ray[1], Kumar Batuk Joshi[1,2,*], S. Sundarraman[1], Deepak Joshi[1] and Talat Ahmad[1,3,*]

[1]Department of Geology, University of Delhi, Delhi 110 007, India
[2]Geoscience Division, Physical Research Laboratory, Ahmedabad 380 009, India
[3]Jamia Millia Islamia, New Delhi 110 025, India

The present study reports the geochemical composition of Sewariya two-mica granites (SG) and Govindgarh granites (GG) intruding rocks of Delhi Supergroup along the western margin of South Delhi Fold Belt in Rajasthan, India. Both granite varieties are highly evolved possessing high SiO_2, Al_2O_3, low MgO, CaO, Fe_2O_3, Ni, Cr and V and are calc-alkaline in nature. In chondrite normalized REE diagrams, SG are characterized by highly fractionated REE patterns (avg La_N/Yb_N = 21.45) and sharp negative Eu anomaly (Eu/Eu* = 0.25), whereas GG do not show significant REE fractionated patterns (avg La_N/Yb_N = 3.31) and have variable Eu anomalies. From primitive mantle normalized multi-element diagrams, crustal signatures (low Nb, Ti and high Pb, U, Th) can be inferred for both the granitoid varieties. Also, strong peraluminous nature, high A/CNK, normative corundum and abundant mica content point towards a (meta)sedimentary protolith for them. An arc setting is indicated by their calc-alkaline nature; volcanic arc or syn-collisional affinities in tectonic discriminant diagrams (Nb versus Y; Rb versus Nb + Y). They are peraluminous leucogranites derived from crustal melts with little mantle contribution as is evident from their mineralogy and geochemical characteristics. The anatectic conditions prevalent during the formation of these granites differed with SG being formed under dehydration conditions, while the formation of GG involved fluid-present melting reactions.

Keywords: Geochemistry; granitoid magmatism, petrography, peraluminous leucogranites.

GRANITOIDS constitute the most abundant rock types in the continental crust and hence have been the subject of manifold discussions regarding their genesis and classification. Granitoid formation includes a variety of processes such as partial melting of crustal components, differentiation and evolution of mantle-derived melts or variable degrees of interaction between them. Different geochemical characteristics of granitic rocks are often attributed to different source-rock compositions; the amount of residual minerals in the magma, varying anatectic conditions or stages of magmatic differentiation. The large varieties of granitoids and processes involved in their formation, compound the complexities associated with their classification and deciphering their origin. Frost *et al.*[1] presented a comprehensive fourfold classification of granitoids, viz. peraluminous leucogranites, Cordilleran granitoids, Caledonian post-orogenic granitoids and A-type granitoids. Most peraluminous leucogranites are considered to be pure crustal melts without any direct mantle contribution[2], or to be residual magmas in which separation of early crystallized phases has occurred[3–6]. Other granitoid varieties result from the hybrid magmas arising from the reaction of supracrustal rocks with mantle-derived melts. Thus, all granitoid magmatism with the exception of peraluminous leucogranites is associated with crustal growth rather than just recycling[7,8].

In the light of recent advances proposed for evolutionary processes responsible for the formation of varieties of granitoids, this study examines the geochemistry and evolution of Govindgarh granitoids (GG) and Sewariya granitoids (SG), which occur along the western margin of the South Delhi Fold Belt (SDFB), intruding rocks of the Delhi Supergroup. Previous geochemical studies of SG are basically confined to major elements and selected trace elements[9–11]. Based on new data, the present study discusses the geochemical characterization of these rocks, classifies SG and GG, and presents better constraints on their genesis.

Geological setting and petrography

The Aravalli–Delhi Fold Belt comprises of supracrustal rocks of Paleoproterozoic Aravalli Supergroup and Meso- to Neo-proterozoic Delhi Supergroup overlying the Archean Banded Gneissic Complex[12,13] basement (~3.5–2.5 Ga), which is considered as the cratonic nucleus of

*For correspondence. (e-mail: tahmad001@yahoo.co.in)

the region[14,15]. The Delhi Supergroup which forms the major lithostratigraphic unit of the Aravalli Range, consists mainly of deep-water to platform-type sediments[16]. Based on the age constraints of the granitoids intruding the Delhi Supergroup[17] and the lithofacies association, Sinha Roy[18] proposed diachronous development of the Delhi Fold Belt, thereby dividing the belt into North Delhi Fold Belt (NDFB) and SDFB. Subsequent geochronological studies suggest that rocks of the Mesoproterozoic NDFB are intruded by older granitoids of ~1.85–1.70 Ga (refs 19–21), whereas the Neoproterozoic SDFB is intruded by younger ~1.0–0.85 Ga granitoids[22–24]. This geochronological division of the granitoids overruled Heron's[25] grouping of all granitoids intruding the Delhi Supergroup as 'Erinpura Granites'. Presently, the term 'Erinpura Granite', in general, refers to the younger granitoids occurring to the southwest of Ajmer city[26] or the granitic, batholithic body occupying Erinpura and neighbouring Sirohi district of Gujarat[27]. Although there are no geochronological constraints on the Sewariya pluton, it is considered to be the largest northern equivalent of Erinpura intrusions[25].

Since our study area is confined to the northern part of SDFB, we follow the classification given by Gupta *et al.*[28], which divides the rocks of Delhi Supergroup of SDFB in its north central part into the Barotiya, Sendra, Bhim and Rajgarh Groups from west to east. The Barotiya and Sendra Groups occupying the western Sendra–Barotiya basin are separated from the Bhim and Rajgarh Groups in the eastern Bhim–Rajgarh basin by an inlier of older pre-Delhi rocks[16]. Based on the nature of volcanics and mineralization associated with them, the Barotiya Group is considered to be a back arc-related rift sequence, whereas the Sendra Group is considered to have origin in an arc-type setting[9,29,30]. Evidence of convergent tectonics has been preserved in form of the Phulad ophiolite suite and blueschist associations in the Basantgarh and Phulad areas of southern Rajasthan[18,31–33]. Rocks with arc affinities have been identified along the length of the Delhi Fold Belt[20,34–38].

Sewariya pluton occurs along the western margin of SDFB and intrudes the Barotiya Group, separating it from the pre-Delhi gneisses (BGC) and overlying Ras Marble occurring in the west (Figure 1). Three phases of the Sewariya batholith, viz. hornblende–biotite granite, biotite-granite and a younger tourmaline leucogranite have been identified[9,10]. The hornblende–biotite granite is considered to be deep level I-type granite, whereas biotite-granite and tourmaline leucogranite are considered as shallow-level orogenic, S-type granites formed by the partial melting of the same source, under different physico-chemical conditions. The biotite granite is volumetrically more abundant, whereas tourmaline leucogranite occurs as pod-like intrusions within the host Barotiya rocks of the Delhi Group[10]. Pandian and Dutta[39] mapped larger exposures of tourmaline leucogranite along the Luni–Sagarmati River in the vicinity of Govindgarh and owing to its distinct characteristics designated it as the Govindgarh granite (Figure 1). Hereafter, we have used the terms Sewariya granites (SG) for the biotite–muscovite granites and Govindgarh granites (GG) for the biotite-absent granites sampled from the Sagarmati River section.

Major mineral assemblage of GG consists of quartz, K-feldspar, plagioclase and muscovite, while tourmaline and garnet occur as accessory phases (Figure 2 *a–d*). Quartz is generally coarse-grained, dominating the thin section and also occurs as fine-grained inclusions and at grain boundaries. A few thin sections also show perthitic texture. Mica occurs as scattered flakes and tourmaline grains are of the schorlite variety showing zoning (Figure 2 *a* and *b*). SG (Figure 2 *e–h*) show similar petrographic characteristics as GG with the difference being that biotite is present in the former and absent in the latter. Also, tourmaline in GG is much coarser-grained and abundant than in SG.

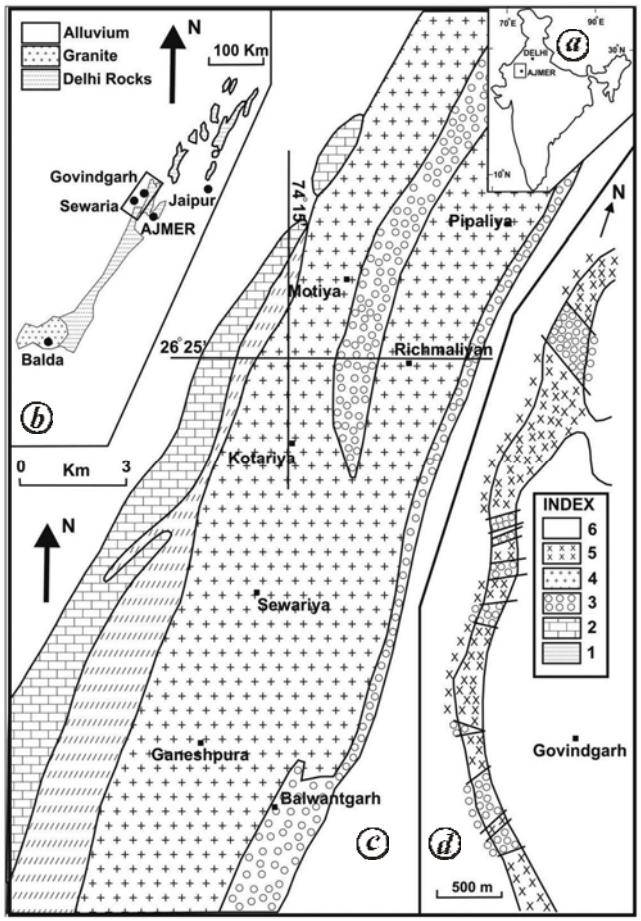

Figure 1. Geological map of the study area. ***a***, Map of India showing the study area; ***b***, Framework of Delhi Fold Belt; ***c***, Geological map of Sewariya area after Bhattacharjee *et al.*[9]; ***d***, Luni–Sagarmati river section near Govindgarh, after Pandian and Dutta[39]. Index: 1, BGC; 2, Ras Marble; 3, Barotiya rocks; 4, Sewariya Granite (SG); 5, Govindgarh granite and 6, Alluvium.

Geochemistry

Systematic sampling was done to collect the most fresh samples of SG and GG from the villages of Sewariya and Govindgarh respectively. A total of 15 samples were collected (8 from GG; 7 from SG) and their chemical analysis was carried out at the National Geophysical Research Institute, Hyderabad. Major elements were analysed using X-Ray fluorescence spectrometry (Phillips MAGIX PRO model 2440) within 3% relative standard deviation[40]. Trace elements (including REE) were determined using inductively coupled plasma mass spectrometer (Perkin Elmer ELAN DRC II) and precision was better than 5% for majority of the trace elements and up to 10% for a[41]. Table 1 gives the major and trace element data of the granitoid samples.

SG and GG show similar abundances of major elements with high SiO_2 (GG_{avg} – 71.3%; SG_{avg} – 72.6%), Al_2O_3 (GG_{avg} – 17.5%; SG_{avg} – 15.4%), low concentrations of MgO, CaO, Fe_2O_3 and high normative corundum. Major elements do not show any well-defined trend with silica in Harker bivariate plots (not shown here), indicating the negligible effects of mineral fractionation on silica content. SG show consistent potassic character with average K_2O/Na_2O value of 1.82, whereas GG are predominantly sodic and have significantly lower TiO_2. In the Ab–An–Or diagram (Figure 3), SG plot within the granite field, whereas GG show granitic to trondhjemitic affinities. All samples are calc-alkaline, strongly peraluminous, ferroan when plotted in the $FeO^t/(FeO^t + MgO)$ diagram (Figure 4 *a*) and range from calc-alkalic to alkali-calcic in the MALI versus SiO_2 diagram (Figure 4 *b*) of Frost *et al.*[1].

Trace element data reveal a distinction between the rocks, wherein GG have lower ∑REE content (avg. 19.26 ppm) than SG (avg. 60.67 ppm). In chondrite normalized REE patterns (Figure 5), SG show somewhat uniform behaviour with highly fractionated REE patterns (avg. $La_N/Yb_N = 21.45$) and sharp negative Eu anomaly ($Eu/Eu^* = 0.25$). On the other hand, GG do not show significant REE fractionated patterns (avg. $La_N/Yb_N = 3.31$) and have variable Eu anomaly. In the mantle normalized multi-element spidergram (Figure 6), GG show HREE enrichment, whereas SG show depletion of HREE. But both the granite groups show negative Nb, Ti and positive U, Th, Pb anomalies. Geochemical signatures of granitoids can be utilized in various discrimination diagrams to infer their tectonic setting and probable evolutionary history. In tectonic discrimination diagrams of Pearce *et al.*[42] (Figure 7 *b*), SG plot within the collisional granite field, whereas GG straddle the boundary of the volcanic arc granite) and syn-collisional granite (syn-COLG) fields.

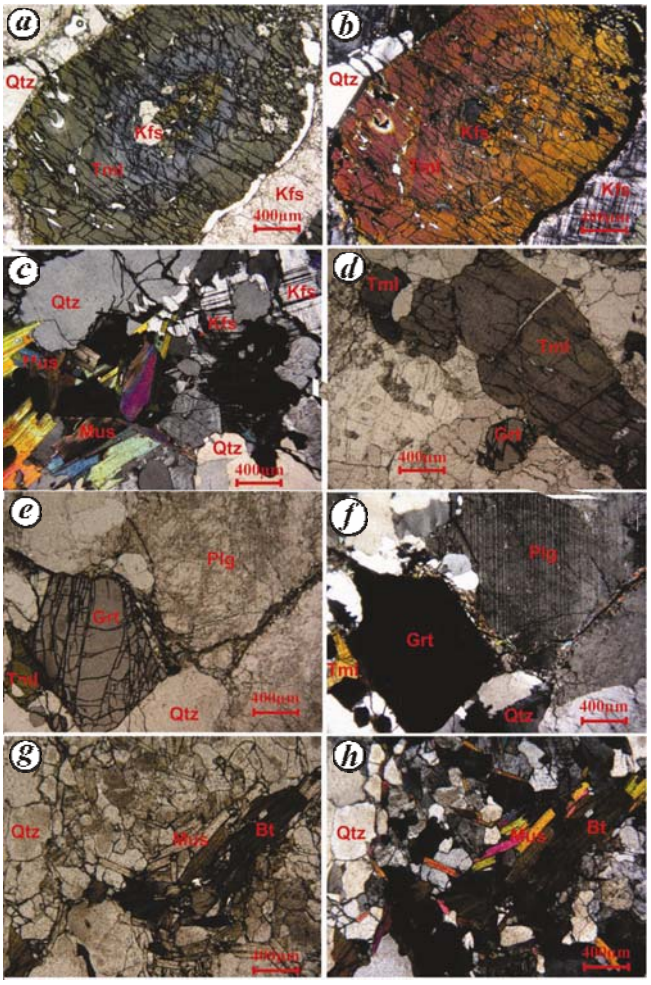

Figure 2. Photomicrographs of (***a***–***d***) Govindgarh and (***e***–***h***) Sewariya granites. Qtz, Quartz; Kfs, K-feldspar; Plg, Plagioclase; Mus, Muscovite; Bt, Biotite; Tml, Tourmaline and Grt, Garnet.

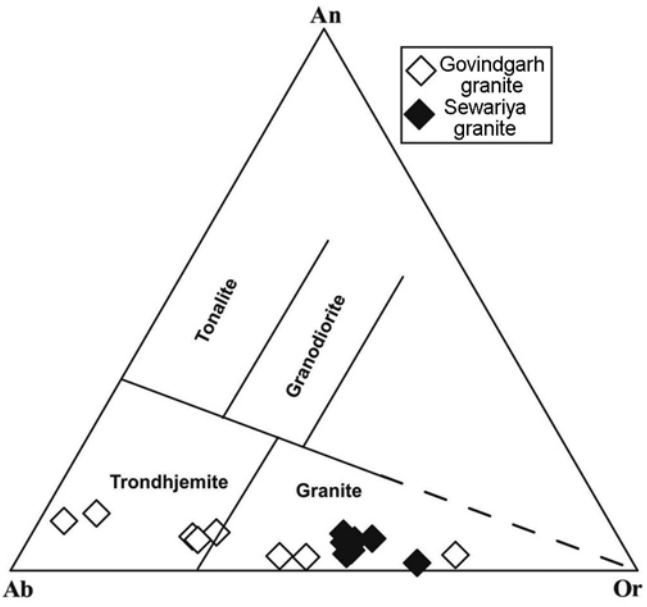

Figure 3. CIPW normative compositions of Govindgarh and SG in Ab–An–Or diagram of O'Connor[55] with fields after Barker[56]. SG show exclusive granitic composition, whereas composition of GG ranges from granitic to trondhjemitic.

Table 1. Major and trace element data of Govindgarh and Sewariya granites

	Govindgarh granite								Sewariya granite						
	D3S1	D3S3	D3S4	D3S9	D3S15	D3S16	D3LS	D3LG	D5S1	D5S3	D5S8	D7S4	D7S6	D7S10	D7S11
SiO_2	67.7	66.9	72.9	72.4	71.6	72.7	73.4	72.9	70.6	73.0	70.5	71.7	75.7	72.5	74.2
TiO_2	0.01	0.02	0.01	0.02	0.03	0.01	0.02	0.01	0.11	0.04	0.09	0.12	0.09	0.14	0.12
Al_2O_3	16.6	21.0	16.9	16.8	17.9	17.0	16.9	16.9	15.9	16.9	15.5	15.5	13.9	15.6	14.4
Fe_2O_3	0.31	0.18	0.48	2.83	1.07	0.69	0.24	0.28	1.68	0.48	2.06	1.92	1.26	1.92	1.41
MnO	0.02	0.06	0.06	0.33	0.05	0.01	0.06	0.03	0.02	0.01	0.02	0.03	0.02	0.03	0.02
MgO	0.05	0.02	0.02	0.11	0.12	0.12	0.02	0.05	0.22	0.02	0.11	0.36	0.14	0.38	0.34
CaO	0.73	1.82	0.86	1.04	0.93	0.8	0.53	0.44	0.94	0.34	0.67	0.76	0.55	0.78	0.88
Na_2O	2.75	7.18	4.38	4.95	4.18	4.23	3.49	3.45	2.9	2.18	3.43	2.95	2.51	2.62	2.71
K_2O	9.91	1.07	2.4	0.32	2.76	2.43	3.72	4.4	5.78	5.81	5.7	4.84	4.3	4.62	4.43
P_2O_5	0.18	0.17	0.13	0.12	0.11	0.15	0.19	0.12	0.15	0.14	0.2	0.13	0.14	0.15	0.12
Sum	98.53	98.52	98.51	101.55	99.65	98.70	98.81	98.77	99.74	99.29	100.09	100.04	99.68	100.53	99.81
Rb	321	67	72	10	94	160	141	160	385	424	410	329	328	396	213
Ba	199	31	69	40	64	62	81	208	189	61	84	75	44	79	106
Th	1	2	1	3	2	3	1	1	15	9	15	10	9	15	7
U	1	1	2	3	3	3	1	2	5	6	2	3	3	6	2
Nb	1	9	3	1	1	1	9	2	6	8	1	7	7	10	4
Pb	144	61	84	69	73	97	78	137	56	51	47	54	29	33	47
Sr	84	67	48	39	31	37	35	69	46	23	19	17	13	22	22
Nd	2	4	3	7	3	2	2	1	15	5	20	8	7	12	8
Zr	22	10	29	88	30	25	10	25	45	32	35	42	27	57	23
V	4	3	3	6	6	5	4	3	5	3	6	7	4	9	5
Ni	4	8	8	9	8	7	8	7	6	3	4	6	4	8	4
Ga	10	14	10	9	10	14	10	9	17	15	18	14	13	16	10
Cs	13	7	4	2	8	13	13	18	25	28	32	25	23	36	16
La	2.26	5.23	3.57	8.34	3.68	2.63	1.97	1.67	16.23	4.69	22.72	8.43	6.69	13.09	9.41
Ce	4.56	10.78	7.23	16.10	7.70	5.94	3.87	2.99	36.79	11.47	44.96	19.96	15.57	29.86	19.22
Pr	0.50	1.09	0.72	1.79	0.83	0.65	0.42	0.32	3.93	1.33	5.61	2.17	1.70	3.26	2.17
Nd	1.80	3.94	2.61	6.56	2.81	2.23	1.51	1.03	15.31	4.96	20.14	8.27	6.50	12.46	8.11
Sm	0.51	0.99	0.67	1.75	0.75	0.67	0.40	0.27	3.98	1.85	4.82	2.37	1.99	3.25	2.04
Eu	0.47	0.34	0.22	0.27	0.18	0.11	0.21	0.42	0.45	0.18	0.19	0.16	0.10	0.22	0.23
Gd	0.41	0.61	0.53	1.51	0.61	0.60	0.31	0.23	3.33	1.83	3.54	1.99	1.65	2.87	1.63
Dy	0.59	0.64	0.87	2.26	0.92	0.93	0.68	0.50	3.66	2.68	3.77	2.27	2.11	3.37	1.68
Er	0.17	0.27	0.44	1.31	0.31	0.26	0.31	0.28	0.60	0.37	0.62	0.41	0.34	0.61	0.31
Yb	0.31	0.60	1.27	4.16	0.72	0.43	0.71	0.78	0.45	0.30	0.47	0.37	0.26	0.48	0.28
Lu	0.06	0.11	0.22	0.75	0.12	0.07	0.12	0.14	0.06	0.03	0.06	0.05	0.03	0.07	0.04
∑REE	11.81	24.82	18.65	45.64	18.87	14.77	10.71	8.79	85.77	30.34	107.94	47.07	37.51	70.45	45.58
$(La/Yb)_N$	5.15	6.25	2.02	1.44	3.66	4.43	2.00	1.55	26.04	11.33	34.45	16.39	18.48	19.44	24.02
(Eu/Eu*)	3.06	1.23	1.08	0.49	0.81	0.50	1.77	5.02	0.37	0.29	0.14	0.22	0.16	0.21	0.37
$(La/Sm)_N$	2.85	3.41	3.42	3.07	3.17	2.54	3.203	4.08	2.63	1.64	3.04	2.30	2.18	2.60	2.98
A/CNK	1.00	1.29	1.48	1.62	1.55	1.54	1.57	1.50	1.24	1.60	1.19	1.35	1.42	1.46	1.32

Major oxides are in wt% and trace elements in ppm.

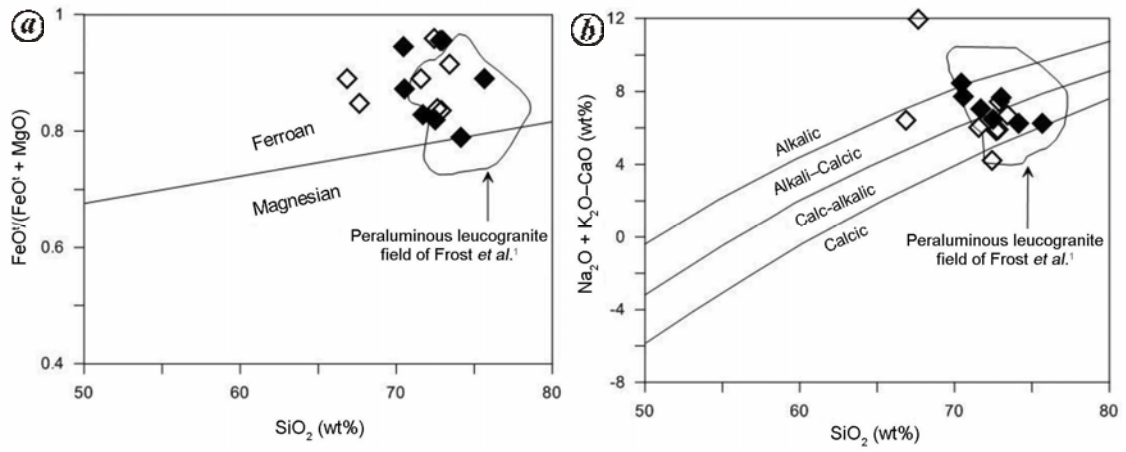

Figure 4. ***a***, Fe number diagram. ***b***, MALI versus SiO_2 diagram for GG and SG. The field denotes peraluminous leucogranites of Frost *et al.*[1]. SG and GG plot well within or in close proximity to peraluminous leucogranites.

Discussion

Granitoids from Sewariya are mainly granites, whereas those from Govindgarh range from granite to trondhjemite in composition according to the Ab–An–Or diagram. SG and GG do not seem to be related through fractional crystallization processes as suggested by lack of well-defined trends on Harker variation plots (not shown here). However, intra-group fractionation cannot be ruled out. The evolved major elemental composition, molar A/CNK > 1.1 (except one GG sample with A/CNK = 1), high normative corundum, and abundant mica content indicate their S-type character[43,44] and strongly suggest a (meta) sedimentary protolith. According to the classification of Frost *et al.*[1], these granitoids are peraluminous leucogranites owing to their strongly peraluminous nature, high silica content, ferroan and calc-alkalic to alkali-calcic character (Figure 4 *a* and *b*) and are thus derived from the crust without any significant contribution from the mantle. This is also reflected in very low FeO, MgO, TiO_2, Ni, Cr, V content and absence of pyroxenes or amphiboles. Additionally, Ce/Pb and Nb/U ratios similar to upper continental crust[45] (UCC) and bulk continental crust[46] (BCC) indicate that they are formed from crustal melts (Figure 8).

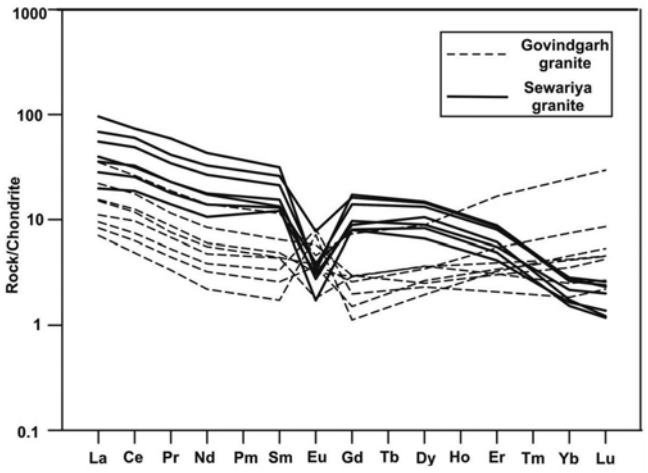

Figure 5. Chondrite normalized REE patterns for GG and SG. While SG are characterized by highly fractionated REE patterns and sharp negative Eu anomaly, GG show HREE enrichment and variable Eu anomalies (from weakly negative to positive). Chondrite elemental values are taken from Sun and McDonough[57].

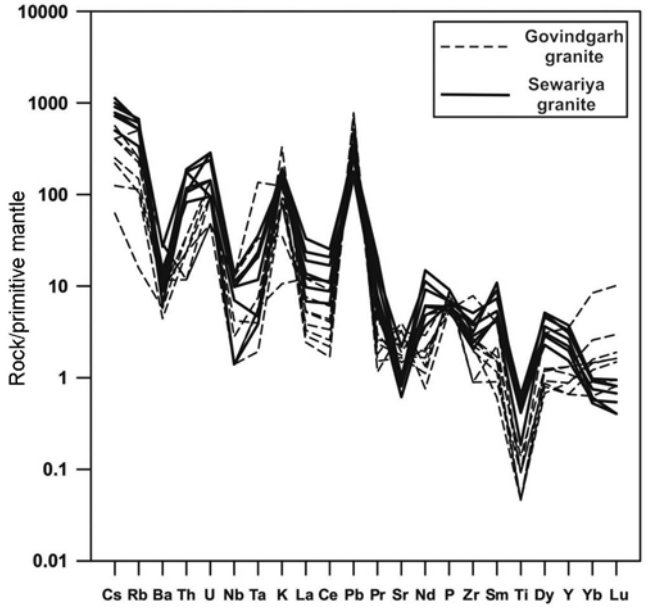

Figure 6. Primitive mantle normalized multi-element spidergrams for GG and SG. Enrichment of K, Rb, Pb, U and depletion of Nb, Ti indicate crustal signatures. High LILE/HFSE ratio and Nb depletion also indicate an arc setting. Primitive mantle elemental values are taken from Sun and McDonough[57].

In chondrite normalized REE diagrams, sharp Eu anomalies for SG point towards plagioclase fractionation and retention of the same at the source. Consistent HREE enrichment in both chondrite normalized and mantle normalized element diagrams, lower La/Yb (avg. – 4.62) and Gd/Yb (avg. – 0.76) values for GG suggest lesser amount of residual garnet in its source than that of SG (HREE depletion; La/Yb_{avg} – 29.90; Gd/Yb_{avg} – 6.37). Crustal signatures are indicated by enrichment of K, Rb, Pb, U, Th and depletion of Nb, Ti (Figure 6). Pronounced Nb depletion could also reflect affinity to subduction zone granitoids and their emplacement in the volcanic arc[37,47,48]. SG and GG show classical patterns for subduction-related rocks and are characterized by high LILE/HFSE ratios and conspicuous negative Nb, Sr (except few samples of GG) and Ti anomalies. Sr, Ti depletion could also result from feldspar and rutile, titano-magnetite fractionation respectively. For GG, however, both Sr enrichment and slight depletion are in agreement with similar dual behaviour shown by Eu, indicating the role of feldspar which has high K_d for both elements. Calc-alkaline nature, subductional geochemical signatures (Figure 6) along with the VAG and syn-collisional signatures (Figure 7) of the granitoids thereby corroborate Sinha Roy's proposition[26] that the Sewariya batholith developed in response to subduction processes. It is absolutely imperative to note that geochemical signatures of granitoids indicate their source-rock compositions and do not circumscribe them to particular tectonic environments[42]. For example, a granitoid formed in a subduction setting may have similar geochemical characters to another granitoid whose protolith was originally derived in a similar setting but subsequently remobilized by crustal extension or rifting.

Crustal-derived melts are generally the products of incongruent melting of micas (especially muscovite) as they provide the lowest temperature conditions at which melts can be generated from a crustal source in fluid absent conditions[49]. Fluid-present melting, on the other hand, consumes plagioclase in greater proportion as the

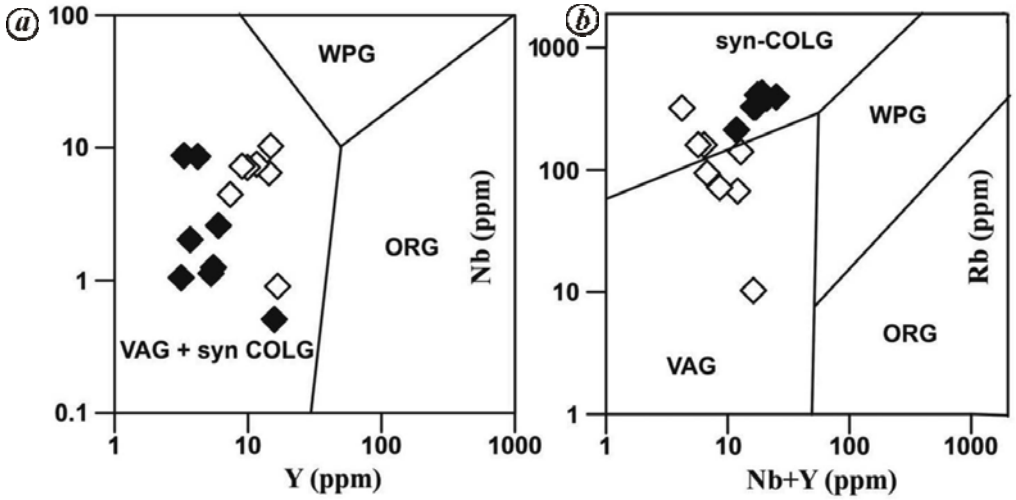

Figure 7. Tectonic discrimination diagrams of Pearce *et al.*[42] for GG and SG. VAG, Volcanic Arc Granites; syn, COLG, Collisional granites; WPG, Within plate Granites; and ORG, Ocean ridge Granites.

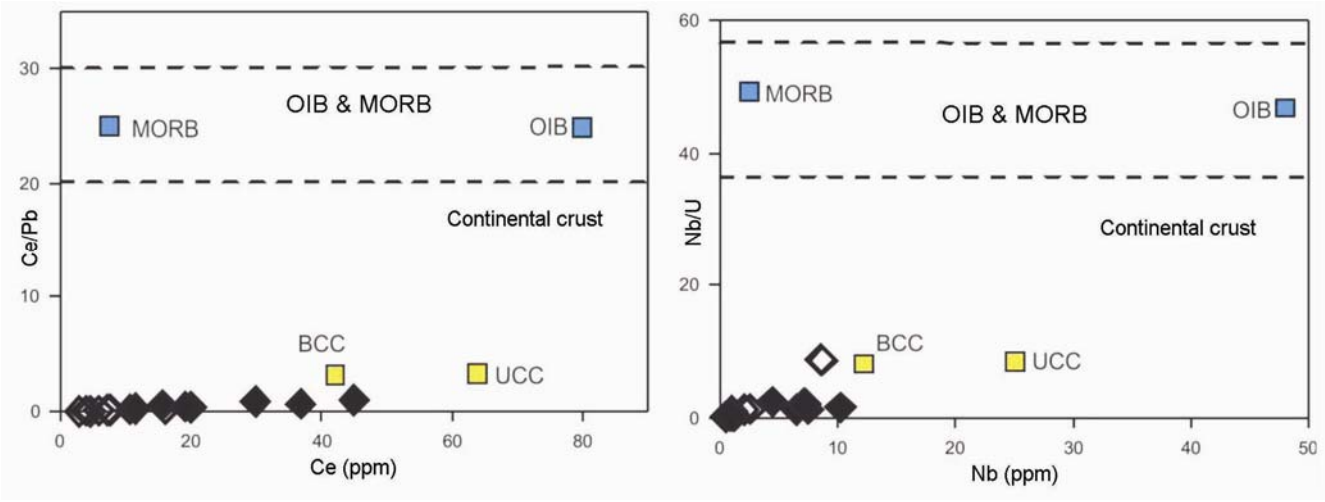

Figure 8. Ce/Pb versus Ce and Nb/U versus Nb plots (after Guo and Wilson[58]). Data for MORB and OIB are from Sun and McDonough[57]; upper continental crust (UCC) from Taylor and McLennan[45], and bulk continental crust (BCC) from Rudnick and Fountain[46]. Similar Ce/Pb and Nb/U values of SG, GG and UCC, BCC imply the former to be crustal melts.

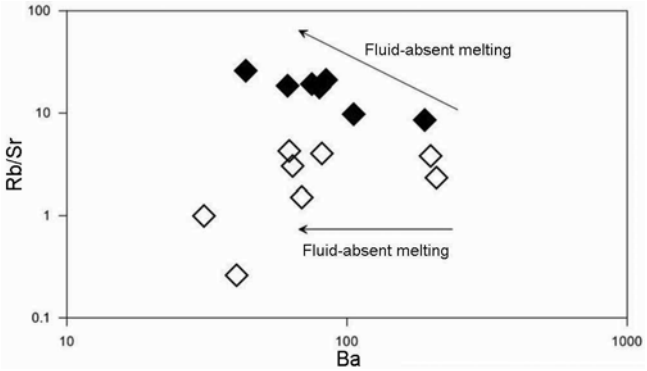

Figure 9. Rb/Sr versus Ba plot for SG and GG. Fluid-present and fluid-absent melting trends are from Inger and Harris[54]. SG follow the fluid-absent melting trend, while GG formed under fluid-present conditions.

plagioclase + quartz solidus is depressed much more than mica solidus[2,50,51] by fluid activity and forms near solidus melts of trondhjemitic composition[2] due to release of Na by plagioclase breakdown. Experimental studies have shown that biotite is a product of muscovite dehydration melting. As opposed to this, in fluid-present melting reactions[2], biotite stability is maximum at reduced fluid activity[52] and low Ti contents in the melt stabilize tourmaline with respect to biotite[53]. In Figure 9, increasing Rb/Sr for decreasing values of Ba in the case of SG could imply muscovite dehydration breakdown. Low melt fractions and restitic K-feldspar contribute to such trends, because low degrees of partial melting result in increasing Rb/Sr and the partition coefficient of K-feldspar for Ba is high[54]. GG, however, could be generated under fluid-present

melting conditions, which explains the low Rb/Sr, absence of biotite, predominantly sodic character and consequent trondhjemitic composition (Figure 3) and positive or weakly negative Eu, Sr anomalies due to melting of source plagioclase. Considerably low Ti contents in GG may have also facilitated non-formation of biotite and presence of the coarser-grained tourmaline. The diverse composition of GG (viz. granitic to trondhjemitic composition and variable Eu, Sr anomalies) probably reflects variable fluid activities and higher melt fractions during anatexis.

Conclusion

Granitoids could be products of innumerable processes operating individually or in combination. Crustal remelting, subductional processes, mantle inputs and various other processes could result in a wide variety of granitoids. Geochemical signatures of rocks provide insights into the processes involved during rock formation. Based on their geochemical characteristics, SG and GG have been classified as peraluminous leucogranites generated by melting of metasedimentary source developed in an arc setting. As discussed, the lack of any differentiation trends on Harker plots (not shown here) obviates the process of fractional crystallization from a common parental melt. Thus, two mechanisms could account for the formation these granites, viz. (i) products of partial melting of different sedimentary protoliths, or (ii) different melt fractions of similar source rock under variable physico-chemical conditions. Whether or not they are derived from the same metasedimentary source has not been answered in this study solely on the basis of major and trace elements geochemistry and would require further deliberation. However, it is evident that the anatectic conditions prevalent during the origin of these granitoids were disparate.

1. Frost, B. R., Barnes, C. G., Collins, W. J., Arculus, R. J., Ellis, D. J. and Frost, C. D., A geochemical classification for granitic rocks. *J. Petrol.*, 2001, **42**, 2033–2048.
2. Patiño Douce, A. E. and Harris, N., Experimental constraints on Himalayan anatexis. *J. Petrol.*, 1998, **39**, 689–710.
3. Bateman, P. C. and Chappell, B. W., Crystallization, fractionation, and solidification of the Tuolumne intrusive series, Yosemite National Park, California. *Geol. Soc. Am. Bull.*, 1979, **90**, 465–482.
4. Price, R. C., Geochemistry of a peraluminous granitoid suite from Northeastern Victoria, Southeastern Australia. *Geochim. Cosmochim. Acta*, 1983, **47**, 31–42.
5. Anderson, J. L. and Thomas, W. M., Proterozoic anorogenic two-mica granites: Silver Plume and St. Vrain batholiths of Colorado. *Geology*, 1985, **13**, 177–180.
6. Sultan, M., Batiza, R. and Sturchio, N. C., The origin of small-scale geochemical and mineralogic variations in a granite intrusion – a crystallization and mixing model. *Contrib. Mineral. Petrol.*, 1986, **93**, 513–523.
7. Patiño Douce, A. E., What do experiments tell us about the relative contributions of crust and mantle to the origin of granitic magmas? *Geol. Soc. London, Specl Publ.*, 1999, **168**, 55–75.
8. Brown, M., Granite: from genesis to emplacement. *Geol. Soc. Am. Bull.*, 2013, **125**, 1079–1113.
9. Bhattacharjee, J., Fareeduddin and Jain, S. S., Tectonic setting, petrochemistry and tungsten metallogeny of the Sewariya granite in the South Delhi Fold Belt, Rajasthan. *J. Geol. Soc. India*, 1993, **42**, 3–16.
10. Banerji, S. and Pandit, M. K., Lithium and tungsten mineralisation in Sewariya pluton, South Delhi Fold Belt, Rajasthan: evidence for preferential host rock affinity. *Curr. Sci.*, 1995, **69**, 252–256.
11. Pandian, M. S., Late proterozoic acid magmatism and associated tungsten mineralisation in northwest India. *Gondwana Res.*, 1999, **2**, 79–87.
12. Wiedenbeck, M., Goswami, J. N. and Roy, A. B., An ion microprobe study of single zircons from the Amet granite, Rajasthan. *J. Geol. Soc. India*, 1996, **48**, 127–137.
13. Roy, A. B. and Kroner, A., Single zircon evaporation ages constraining the growth of the Archaean Aravalli craton and, northwestern Indian shield. *Geol. Mag.*, 1996, **133**, 333–342.
14. Ahmad, T. and Tarney, J., Geochemistry and petrogenesis of late Archaean Aravalli volcanics, basement enclaves and granitoids, Rajasthan. *Precambrian Res.*, 1994, **65**, 1–23.
15. Tobisch, O. T., Collerson, K. D., Bhattacharyya, T. and Mukhopadhyay, D., Structural relationships and Sr–Nd isotope systematics of polymetamorphic granitic gneisses and granitic-rocks from central Rajasthan, India – implications for the evolution of the Aravalli Craton. *Precambrian Res.*, 1994, **65**, 319–339.
16. Roy, A. B. and Jakhar, S. R., *Geology of Rajasthan (Northwest India), Precambrian to Recent*, Pawan Kumar Scientific Publishers, Jodhpur, India, 2002, p. 421.
17. Choudhary, A. K., Gopalan, K. and Sastry, C. A., Present status of the geochronology of the Precambrian rocks of Rajasthan. *Tectonophysics*, 1984, **105**, 131–140.
18. Sinha Roy, S., Precambrian crustal interaction in Rajasthan, NW India. In Proceedings of the seminar on crustal evolution of Indian shield and its bearing on metallogeny. *Indian J. Earth Sci.*, 1984, pp. 84–91.
19. Biju-Sekhar, S., Yokoyama, K., Pandit, M. K., Okudaira, T. and Santosh, M., Late Paleoproterozoic magmatism in Delhi Fold Belt, NW Indian and its significance: evidence from EPMA chemical ages of zircons. *J. Asian Earth Sci.*, 2003, **22**, 189–207.
20. Kaur, P., Chaudhri, N., Raczek, I., Kröner, A. and Hofmann, A. W., Record of 1.82 Ga Andean-type continental arc magmatism in NE Rajasthan, India: insights from zircon and Sm/Nd ages, combined with Nd–Sr isotope geochemistry. *Gondwana Res.*, 2009, **16**, 56–71.
21. Kaur, P., Chaudhri, N., Raczek, I., Kröner, A., Hofmann, A. W. and Okrusch, M., Zircon ages of late Palaeoproterozoic (ca. 1.72–1.70 Ga) extension-related granitoids in NE Rajasthan, India: regional and tectonic significance. *Gondwana Res.*, 2011, **19**, 1040–1053.
22. Deb, M., Thorpe, R. I., Krstic, D., Corfu, F. and Davis, D. W., Zircon U–Pb and galena Pb isotope evidence for an approximate 1.0 Ga terrane constituting the western margin of the Aravalli–Delhi orogenic belt, northwestern India. *Precambrian Res.*, 2001, **108**, 195–213.
23. Pandit, M. K., Carter, L. M., Ashwal, L. D. and Tucker, R. D., Torsvik, T. H., Jamtveit, B. and Bhushan, S. K., Age, petrogenesis and significance of 1 Ga granitoids and related rocks from the Sendra area, Aravalli Craton, NW India. *J. Asian Earth Sci.*, 2003, **22**, 363–381.
24. Volpe, A. M. and MacDougall, S. D., Geochemistry and isotopic characteristics of mafic (Phulad ophiolite) and related rocks in the Delhi Supergroup. Rajasthan India: implications for rifting in the Proterozoic. *Precambrian Res.*, 1990, **48**, 167–191.
25. Heron, A. M., Geology of central Rajputana. *Mem. Geol. Soc. India*, 1953, 79, pp. 339.

26. Sinha Roy, S., Proterozoic Wilson cycles in Rajasthan. *Mem. Geol. Soc. India*, 1988, **7**, 95–107.
27. Sarkar, S. C. and Gupta, A., *Crustal Evolution and Metallogeny in India*, Cambridge University Press, 2012.
28. Gupta, P., Fareeduddin, R. M. S. and Mukhopadhyay, K., Stratigraphy and structure of Delhi Supergroup of rocks in central part of Aravalli range. *Rec. Geol. Surv. India*, 1995, **120**, 12–26.
29. Bose, U. and Fareeduddin and Reddy, M. S., Polymodal volcanism in South Delhi Fold Belt, Rajasthan. *J. Geol. Soc. India*, 1990, **36**, 263–276.
30. Bhattacharjee, J., Golani, P. R. and Reddy, A. B., Rift related bimodal volcanism and metallogeny in the Delhi fold belt. Rajasthan and Gujarat. *Indian J. Geol.*, 1988, **60**, 191–199.
31. Gupta, S. N., Arora, Y. K., Mathur, R. K., Iqbaluddin, Balmiki Prasad, Sahi, T. N. and Sharma, S. B., Lithostratigraphic map of the Aravalli region, southern Rajasthan and northeastern Gujarat. Geol. Surv. India Publication, Hyderabad, 1980.
32. Sinha-Roy, S. and Mohanty, M., Blueschist facies metamorphism in the ophiolitic melange of the Late Proterozoic Delhi Fold Belt, Rajasthan. *Precambrian Res.*, 1988, **42**, 97–105.
33. Khan, M. S., Smith, T. E., Raza, M. and Huang, J., Geology, geochemistry and tectonic significance of mafic–ultramafic rocks of Mesoproterozic Phulad Ophiolite Suite of South Delhi Fold Belt, NW Indian shield. *Gondwana Res.*, 2005, **8**, 553–566.
34. Sugden, T. J. and Windley, B. F., Geotectonic framework of the early–mid Proterozoic Aravalli-Delhi orogenic belt, NW India. Geol. Assoc. Canada, Program with Abstracts, 1984, vol. 9, p. 109.
35. Deb, M. and Sarkar, S. C., Proterozoic tectonic evolution and metallogenesis in the Aravalli–Delhi orogenic complex, northwestern India. *Precambrian Res.*, 1990, **46**, 115–137.
36. Dharma Rao, C. V., Santosh, M. and Kim, S. W., Cryogenian volcanic arc in the NW Indian shield: SHRIMP U–Pb zircon ages from felsic tuffs and implications for Gondwana assembly. *Gondwana Res.*, 2012, **22**, 36–53.
37. Dharma Rao, C. V., Santosh, M., Kim, S. W. and Li, S., Arc magmatism in the Delhi Fold Belt: SHRIMP U–Pb zircon ages of granitoids and implications for Neoproterozoic convergent margin tectonics in NW India. *J. Asian Earth Sci.*, 2013, **78**, 83–99.
38. Joshi, K. B., Ray, S., Joshi, D. and Ahmad, T., Geochemistry of pegmatites from South Delhi Fold Belt: a case study from Rajgarh, Ajmer District, Rajasthan. *Curr. Sci.*, 2014, **106**, 1725–1730.
39. Pandian, M. S. and Dutta, S. K., Leucogranite magmatism in Sewariya–Govindgarh areas of Rajasthan and its relevance to tungsten mineralisation. *J. Geol. Soc. India*, 2000, **55**, 289–295.
40. Krishna, A. K., Murthy, N. N. and Govil, P. K., Multielement analysis of soils by wavelength-dispersive X-ray fluorescence spectrometry. *At. Spectrosc.*, 2007, **28**, 202–214.
41. Balaram, V. and Rao, T. G., Rapid determination of REEs and other trace elements in geological samples by microwave acid digestion and ICP-MS. *At. Spectrosc.*, 2004, **24**, 206–212.
42. Pearce, J. A., Harris, N. B. W. and Tindle, A. G., Trace element discrimination diagrams for the tectonic interpretation of granitic rocks. *J. Petrol.*, 1984, **25**, 956–998.
43. Chappell, B. W. and White, A. J. R., Two contrasting granite types. *Pac. Geol.*, 1974, **8**, 173–174.
44. Chappell, B. W. and White, A. J. R., Two contrasting granite types: 25 years later. *Aust. J. Earth Sci.*, 2001, **48**, 489–499.
45. Taylor, S. R. and McLennan, S. M., *The Continental Crust: its Composition and Evolution*, Blackwell, Oxford, 1985.
46. Rudnik, R. L. and Fountain, D. M., Nature and composition of the continental crust: a lower crustal perspective. *Rev. Geophys.*, 1995, **33**, 267–309.
47. Roberts, M. P. and Clemens, J. D., Origin of high-potassium, calc-alkaline, I-type granitoids. *Geology*, 1993, **21**, 825–828.
48. White, W. M., *Geochemistry*, Wiley-Blackwell, 2007, p. 413; Online textbook: http://www.geo.cornell.edu/geology/classes/geo455/Chapters.HTML (last revised 21 November 2007).
49. Harris, N., Ayres, M. and Massey, J., Geochemistry of granitic melts produced during the incongruent melting of muscovite: implications for the extraction of Himalayan leucogranite magmas. *J. Geophys. Res.*, 1995, **100**, 15767–15777.
50. Conrad, W. K., Nicholls, I. A. and Wall, V. J., Water-saturated and undersaturated melting of metaluminous and peraluminous crustal compositions at 10 kb: evidence for the origin of rhyolites in the Taupo Volcanic Zone, New Zealand, and other granitoids. *J. Petrol.*, 1988, **29**, 765–803.
51. Patiño Douce, A. E., Effects of pressure and H_2O content on the compositions of primary crustal melts. *Trans. R. Soc., Edinburgh: Earth Sci.*, 1996, **87**, 11–21.
52. Scaillet, B., Pichavant, M. and Roux, J., Experimental crystallization of Leucogranite magmas. *J. Petrol.*, 1995, **36**, 663–705.
53. Nabelek, P., Russ-Nabelek, C. and Denison, J., The generation and crystallization conditions of the Proterozoic Harney Peak leucogranite, Black Hills, South Dakota, USA: petrologic and geochemical constraints. *Contrib. Mineral. Petrol.*, 1992, **110**, 173–191.
54. Inger, S. and Harris, N., Geochemical constraints on leucogranites magmatism in the Langtang Valley, Nepal Himalaya. *J. Petrol.*, 1993, **34**, 345–368.
55. O'Connor, J. T., A classification for quartz-rich igneous rocks based on feldspar ratio. *US Geol. Surv. Prof. Pap. B*, 1965, **525**, 79–84.
56. Barker, F., Trondhjemite: definition, environment and hypotheses of origin. In *Trondhjemites, Dacites and Related Rocks* (ed. Barker, F.), Elsevier, Amsterdam, 1979, pp. 1–11.
57. Sun, S. S. and McDonough, W. F., Chemical and isotopic systematics of oceanic basalts: implications for mantle composition and processes. *Geol. Soc. London, Spec. Publ.*, 1989, **42**, 313–345.
58. Guo, Z. and Wilson, M., The Himalayan leucogranites: constraints on the nature of their crustal source region and geodynamic setting. *Gondwana Res.*, 2012, **22**, 360–376.

ACKNOWLEDGEMENTS. We thank the Head, Department of Geology, University of Delhi for providing the necessary facilities, and scientists from the XRF and ICP-MS Laboratory, NGRI, Hyderabad for analysing the samples. Critical comments from Dr Esa Heilimo helped improve of the manuscript. We also thank the anonymous reviewer for useful suggestions. This is a contribution to IGCP-SIDA project number 599.

Received 12 November 2014; revised accepted 24 July 2015

doi: 10.18520/v109/i8/1458-1465